

Least-Squares-Based Deep Learning for Sentinel-2 Derived Bathymetry A Case Study on Anegada's Southern Coast

Liu, Yushan; Amiri-Simkooei, Alireza; Lindenbergh, Roderik; Snellen, Mirjam

10.5194/isprs-Archives-XLVIII-2-W10-2025-169-2025

Publication date

Document Version Final published version

Published in

International Archives of the Photogrammetry, Remote Sensing and Spatial Information Sciences - ISPRS **Archives**

Citation (APA)

Liu, Y., Amiri-Simkooei, A., Lindenbergh, R., & Snellen, M. (2025). Least-Squares-Based Deep Learning for Sentinel-2 Derived Bathymetry: A Case Study on Anegada's Southern Coast. *International Archives of the Photogrammetry, Remote Sensing and Spatial Information Sciences - ISPRS Archives, 48*(2/W10-2025), 169-176. https://doi.org/10.5194/isprs-Archives-XLVIII-2-W10-2025-169-2025

Important note

To cite this publication, please use the final published version (if applicable). Please check the document version above.

Other than for strictly personal use, it is not permitted to download, forward or distribute the text or part of it, without the consent of the author(s) and/or copyright holder(s), unless the work is under an open content license such as Creative Commons.

Takedown policyPlease contact us and provide details if you believe this document breaches copyrights. We will remove access to the work immediately and investigate your claim.

Least-Squares-Based Deep Learning for Sentinel-2 Derived Bathymetry: A Case Study on Anegada's Southern Coast

Yushan Liu¹, Alireza Amiri-Simkooei², Roderik Lindenbergh³, Mirjam Snellen⁴

Dept. of Control and Operations, TU Delft, 2629 HS Delft, the Netherlands - yliu74@tudelft.nl
Dept. of Control and Operations, TU Delft, 2629 HS Delft, the Netherlands - a.amirisimkooei@tudelft.nl
Dept. of Geoscience and Remote Sensing, TU Delft, 2628 CN Delft, the Netherlands - r.c.lindenbergh@tudelft.nl
Dept. of Control and Operations, TU Delft, 2629 HS Delft, the Netherlands - m.snellen@tudelft.nl

Keywords: Least-squares-based deep learning (LSBDL), Satellite-derived bathymetry (SDB), ICESat-2, Sentinel-2.

Abstract

Satellite-derived bathymetry (SDB) provides a cost-effective solution for coastal mapping, but challenges remain in model interpretability and uncertainty quantification. This study investigates the applicability of the least-squares-based deep learning (LSBDL) framework for SDB, leveraging its hybrid structure that integrates neural networks with the available least-squares theory to enhance model transparency. ICESat-2 photon-counting LiDAR was used to train depth estimation from Sentinel-2 multispectral imagery over an approximately $30\,\mathrm{km} \times 30\,\mathrm{km}$ region of near-coastal bathymetry at Anegada, British Virgin Islands. ICESat-2 provided high-precision depth information, of which 80% were used for training and the remainder for validation. LBSDL depth estimation achieved a root-mean-square error (RMSE) of $2.74\,\mathrm{m}$, representing around 10% of the maximum observed depth, with the best performance in the $2-15\,\mathrm{m}$ depth range. These findings demonstrate the potential of LSBDL for interpretable and reliable bathymetric mapping, highlighting ICESat-2 as a globally accessible training and validation source and advancing SDB capabilities for data-sparse coastal regions.

1. Introduction

Bathymetric mapping of shallow coastal waters is essential for navigational safety, environmental monitoring, and coastal infrastructure planning. Traditional methods such as echo sounding and airborne light detection and ranging (LiDAR) offer high accuracy but are often constrained by high cost, limited coverage, and logistical challenges (Bernardis et al., 2023). As an alternative, satellite-derived bathymetry (SDB) provides a scalable, cost-effective means of estimating depth by exploiting light attenuation in clear water using multispectral imagery. This method facilitates rapid and frequent mapping of shallow zones where in-situ data are sparse or unavailable.

A wide range of SDB approaches have been developed, broadly categorized into empirical and physics-based models (Ashphaq et al., 2021). Physics-based inversion methods estimate depth by modeling the light propagation physic (Kim et al., 2024) or by analyzing wave kinematics (Najar et al., 2022; Al Najar et al., 2023). These methods, in principle, allow depth retrieval without local depth samples. However, such methods often neglect some environmental influences and require detailed knowledge of site-specific optical properties, which complicates their general applicability. They can also be limited by the spectral capabilities of the available imagery, particularly the need for sufficient blue—green band sensitivity (Niroumand-Jadidi et al., 2020).

Empirical methods, in contrast, rely on statistical relationships between multispectral reflectance and water depth, commonly implemented through band ratio techniques or multilinear regression models (Eugenio et al., 2021). These models are computationally efficient and easy to apply but typically require calibration with in-situ depth measurements, which limits their applicability in remote and data-sparse areas. Recent studies have addressed this limitation by leveraging satellite LiDAR

data from ICESat-2 as a viable source of reference bathymetric data. Accurate bathymetric points can be derived from the ICESat-2 photon-counting laser altimeter, which can serve as calibration data for SDB models (Ma et al., 2020). Replacing field measurements with ICESat-2 depths enables fully satellite-based workflows for bathymetry, greatly expanding the reach of empirical SDB to areas previously lacking reference data. However, these methods have been simplified to a large extent, which limits their performance to capture spatially complex depth variations over larger areas.

Over the last decade, machine learning (ML) techniques have increasingly been adopted to improve SDB by capturing complex, nonlinear relationships between spectral data and depth. A variety of ML models, including neural networks (NNs), support vector machines (SVMs), random forest (RF), and deep learning (DL) models, have demonstrated promising performance in this domain (Xie et al., 2024). These data-driven methods can extract high-dimensional features from imagery and do not require strict physics-based correction, such as detailed atmospheric corrections or water column parameters. In particular, convolutional neural networks (CNNs) can exploit the spatial context of pixels, such as the similarity of neighboring reflectance and depth, to enhance bathymetric estimation accuracy (Xie et al., 2024). Nevertheless, conventional ML/DL models function largely as "black boxes" that fit statistical patterns in the data while disregarding the physical processes, which can raise concerns about interpretability and reliability.

In this work, we explore a novel least-squares-based deep learning (LSBDL) approach to SDB, which integrates the predictive capabilities of deep neural networks with the statistical transparency of classical least-squares estimation. LSBDL, recently introduced by Amiri-Simkooei et al. (2024), is an emerging paradigm that reformulates a deep learning model within the framework of least-squares theory. In an LSBDL model, the

neural network is trained to construct the design matrix for a linear(ized) model relating input to output. The design matrix is determined through an iterative procedure using the least-squares optimization techniques such as steepest descent or the Gauss–Newton method. This allows the network to handle and train the nonlinear feature patterns, while the final prediction step remains a linear least-squares solution that inherits all the well-established statistical tools of that framework. A key advantage of LSBDL is thus its interpretability. For example, one can directly compute quality measures like the covariance matrix of the predicted outcomes. As a result, uncertainty estimates for the predicted depths are inherently produced as part of the model output, in contrast to conventional deep learning models, which typically lack native uncertainty quantification.

We apply the LSBDL framework to derive bathymetry around Anegada, British Virgin Islands—a coral reef environment—using only freely available satellite data. Specifically, Sentinel-2 multispectral imagery is used as input, while ICESat-2 LiDAR-derived depths serve as training targets. Preliminary results show that our LSBDL model achieves an overall depth estimation root-mean-square error (RMSE) of about 2.74 m, with the best performance across the 2-15 m depth range. These findings highlight the potential of LSBDL to produce accurate and interpretable bathymetric maps for shallow waters, while taking advantage of the global accessibility of satellite data and the statistical rigor of least-squares theory.

The remainder of this paper is organized as follows. Section 2 describes the datasets used in this study. This includes Sentinel-2 multispectral imagery and ICESat-2 LiDAR data, along with an overview of the study area around Anegada Island. Section 3 outlines the overall workflow of the study and introduces the two primary methodologies: the bathymetry retrieval approach and the least-squares-based deep learning (LSBDL) model. Section 4 presents the experimental results, while Section 5 provides a discussion of the findings. Finally, Section 6 concludes the paper and offers directions for future research.

2. Data and Study Area

2.1 Study area: Anegada island

In this study, the area of interest is Anegada Island, the northernmost of the British Virgin Islands (BVI), located in the northeastern Caribbean Sea. Unlike the other volcanic islands within the BVI archipelago, Anegada is primarily composed of coral and limestone, which makes it geologically unique and exceptionally low-lying. With a maximum elevation barely exceeding 8.5 m above the sea level, the island's exposed landmass spans approximately 24 km in length and 5 km in width, covering an area of about 38 km².

The defined rectangular study region surrounding Anegada Island covers an area of approximately $30\,\mathrm{km} \times 30\,\mathrm{km}$, bounded by latitudes $18.6527^\circ - 18.7683^\circ\mathrm{N}$ and longitudes $64.4305^\circ - 64.2687^\circ\mathrm{W}$. The southern coast of Anegada exhibits a depth range from $0\,\mathrm{m}$ to approximately $40\,\mathrm{m}$. The combination of low turbidity and gradual depth increase makes this region an ideal environment to evaluate the performance of the proposed LSBDL model.

As illustrated in Figure 1, the study area is intersected by eight ICESat-2 ground tracks per year for both 2022 and 2023, making in total 16 tracks. These tracks span both the terrestrial

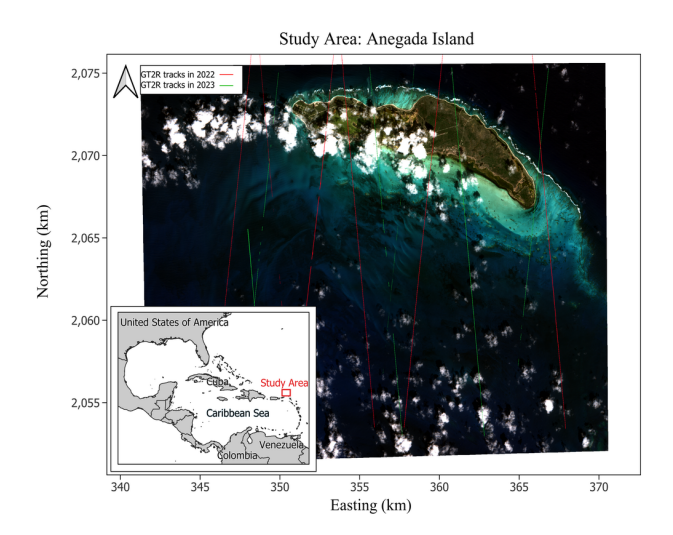


Figure 1. Anegada Island overlaid with 16 ICESat-2 beam patterns on Sentinel-2 imagery from 11/10/2023. Beam tracks from 2023 are in green, and those from 2022 in red (8 per year). Coordinates are in kilometers (EPSG:32620, WGS 84 / UTM zone 20N).

area of the island and its southern coastal waters. They provide sufficient coverage for accurate depth prediction throughout the region.

2.2 Sentinel-2 satellite imagery

Sentinel-2 imagery was selected for depth retrieval around Anegada Island due to its high spatial resolution, wide spectral coverage, frequent revisit capability, and free availability. The Sentinel-2 mission, operated by the European Space Agency (ESA), provides multispectral optical data in 13 bands ranging from the visible to the shortwave infrared (SWIR), with spatial resolutions of 10 m, 20 m, and 60 m depending on the band. For this study, Level-2A (L2A) surface reflectance products were used, which include atmospheric corrections and cloud masking, making them suitable for shallow water and land surface analysis. The combination of fine resolution, coastal-relevant bands, and high temporal frequency (every five days at the equator with both Sentinel-2A and 2B) makes Sentinel-2 particularly valuable for monitoring dynamic coastal environments like those surrounding Anegada.

In this study, we primarily used a Sentinel-2 image acquired on 11 October 2023. This date was selected based on favorable acquisition geometry, including an off-nadir viewing angle of less than 30°, a sun elevation between 30–60°, and an off-set azimuth, providing optimal illumination and viewing conditions (European Space Agency, 2015). Since the focus is on data from 2023, this scene was chosen from several candidates meeting those criteria. As shown in Figure 2, some cloud coverage is present but was effectively masked using the Scene Classification Layer (SCL) band during preprocessing. Band 10 is missing from this dataset; however, its absence is not considered significant, as it has a coarse spatial resolution (60 m) and a central wavelength at 1375 nm, which is primarily used for cirrus cloud detection and does not contribute to water penetration or shallow water analysis.

2.3 ICESat-2 LiDAR dataset

ICESat-2, the Ice, Cloud, and land Elevation Satellite-2, was launched by the National Aeronautics and Space Administra-

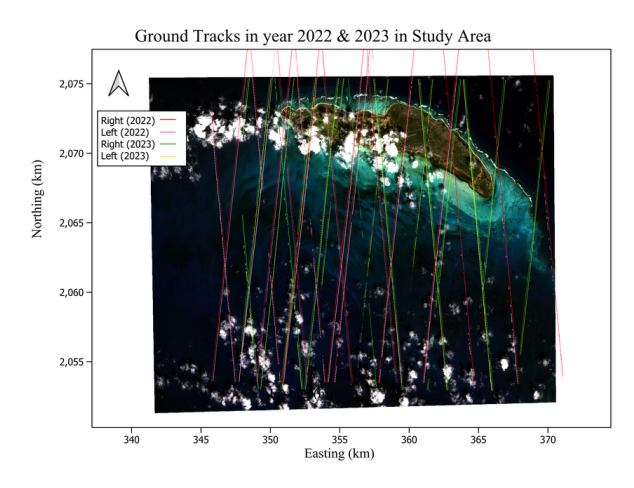


Figure 2. Basemap of study area based on Sentinel-2 imagery from 11/10/2023. Indicated also all ICESat-2 88 ground tracks (6 per beam pattern, with some missing). Tracks from 2023 are in green and yellow; 2022 in red and pink. Coordinates are in kilometers (EPSG:32620, WGS 84 / UTM zone 20N).

tion (NASA) in 2018. It provides high-resolution elevation data through its Advanced Topographic Laser Altimeter System (AT-LAS). ATLAS uses photon-counting LiDAR in combination with precise geolocation from global positioning system (GPS), star cameras, and onboard processing. As ICESat-2 orbits the Earth, ATLAS emits laser pulses that are split into three beam pairs, each consisting of a strong and a weak beam. This results in six approximately 14 m-wide laser footprints across the ground track swath. These laser footprints are arranged as Ground Tracks (GT) 1, 2, and 3, each with left (L) and right (R): GT1L, GT1R, GT2L, GT2R, GT3L, and GT3R. This six-beam configuration is often referred to as the "beam pattern" or "laser footprint array" along the satellite's orbital path, called also the reference ground track. In some instances, one or more beams may be missing due to signal dropout or acquisition anomalies. Figure 3 illustrates the spatial arrangement of the six beams relative to the satellite's track.

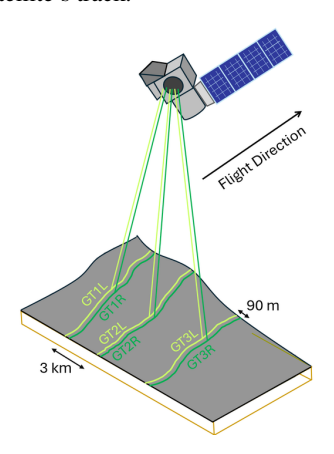


Figure 3. Beam pattern for ICESat-2. Light green beams are relatively low energy (weak) beams; dark green indicates relatively high energy (strong) beams.

The ICESat-2 dataset typically includes 8 beam patterns per year, yielding about 48 ground tracks and approximately 20,000 labeled data points annually when matched with Sentinel-2 imagery at 10-meter resolution. However, this size of dataset proved insufficient for the LSBDL model, which exhibited per-

sistent underfitting—marked by high training error and failure to capture spatial patterns—even after extensive hyperparameter tuning. The core issue is the sparse spatial distribution of individual beam patterns. To enhance spatial coverage without introducing unnecessary redundancy, we incorporated data from both 2022 and 2023. As illustrated in Figure 2, this increased the number of ground tracks intersecting the island to approximately 88, substantially improving coverage, especially in the critical southern coastal region.

3. Methodology

In this study, we followed a structured workflow to apply LS-BDL for SDB, starting with data preprocessing. For Sentinel-2 imagery, the preprocessing involved converting reflectance values, masking non-water pixels, and normalizing spectral bands. ICESat-2 data underwent a series of corrections including noise filtering, geoid and atmospheric adjustments, and refraction correction. From the corrected ICESat-2 dataset, bathymetric profiles were extracted to obtain depth measurements. The depth values were then co-registered with the Sentinel-2 image at a 10-meter resolution. After the data cleaning steps, they were split into training and validation sets. The LSBDL model was trained using the prepared training data, and subsequently was applied to predict bathymetry on the validation subset. Finally, model performance was assessed through error analysis. The complete end-to-end pipeline for this LSBDL-based SDB approach is illustrated in the diagram in Figure 4. We first introduce the methodology used for bathymetry extraction using ICESat-2 data. We then present the LSBDL model, detailing its structure and the procedures for training and prediction.

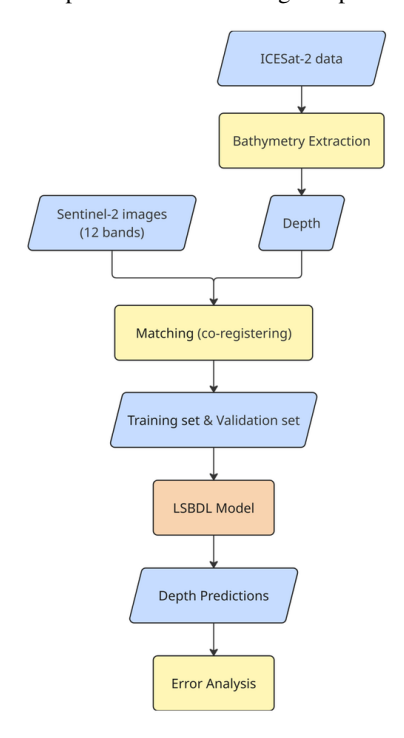


Figure 4. Workflow for LSBDL-based satellite-derived bathymetry (SDB) using Sentinel-2 and ICESat-2 data.

3.1 Bathymetry extraction from ICESat-2 data

The geolocated seafloor photon returns from ICESat-2 data cannot be directly used as bathymetric measurements because the

171

standard ICESat-2 data products do not account for the refraction that occurs at the air—water interface. Therefore, a dedicated post-processing step is required to produce accurate bathymetric estimates. In this study, we implemented the photon-based refraction correction methodology developed by Parrish et al. (2019). In their validation over the U.S. Virgin Islands using airborne bathymetric LiDAR, this method achieved vertical root mean square errors (RMSEs) of around 0.43 m.

Our workflow begins with the ATL03 geolocated photon data. An initial filtering step is applied using the YAPC (Yet Another Photon Classifier) density-based score (Sutterley, 2023) to assign a confidence value to each photon. A threshold is then applied to exclude noise photons, and this is further refined by incorporating the photon weights available in the ICESat-2 metedata. The water surface is extracted by identifying the most frequent elevation value among the surface-return photons. To facilitate efficient along-track analysis, the photon cloud is binned into a vertical histogram at a resolution defined by the ATL03 segment bin size. Bottom-return photons are then identified by detecting the second peak in the vertical histogram, which is expected to correspond to seafloor reflections from below the water surface. Once the bottom photons are segmented, the refraction correction algorithm is applied to determine the depth. An example of refraction-corrected bathymetry is illustrated in Figure 5.

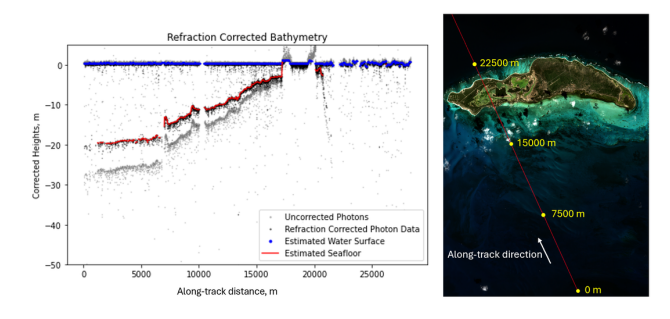


Figure 5. Example of extracted bathymetry from ICESat-2 ground track ATL03_20220808011200_07201601_006_01 GT2R (left), and the corresponding ground track overlaid on Sentinel-2 imagery from 30/12/2023 (right).

The refraction correction method relies on known or assumed values for the refractive indices of air and water. For each photon, the algorithm computes the corrected position in three dimensions by calculating the difference between the apparent and true locations of the seafloor return. This involves estimating the slant path through the water column and adjusting for the change in light direction and speed due to refraction. The method is computationally efficient and accounts for Earth curvature when needed. This allows accurate bathymetric estimation even from near-nadir observations.

3.2 Least-squares-based deep learning model

Least-squares-based deep learning (LSBDL) is adopted here as a novel framework that combines the interpretability of linear least-squares models with the predictive power of deep neural networks. As illustrated in Figure 6, the LSBDL training pipeline feeds the input features through a nonlinear activation layer and then computes the output weights by solving a Tikhonov-regularized least-squares problem (ridge regression) to model the reference depths. The initial depth prediction is compared to the ICESat-2-derived target, yielding a residual error \hat{E} . LS-BDL can in principle apply back-propagation of this error through

multiple layers. For a single-layer model, LSBDL uses the residual to directly update the hidden-layer weight matrix W in a forward manner, and then recomputes the global optimal output weights X in the next iteration. This iterative residual-based update continues until convergence, which ensures that each weight adjustment is explicitly tied to reducing the prediction error. Consequently, the training process is more transparent and interpretable than that of a conventional deep network, because it is formulated in the framework of the existing least-squares theory.

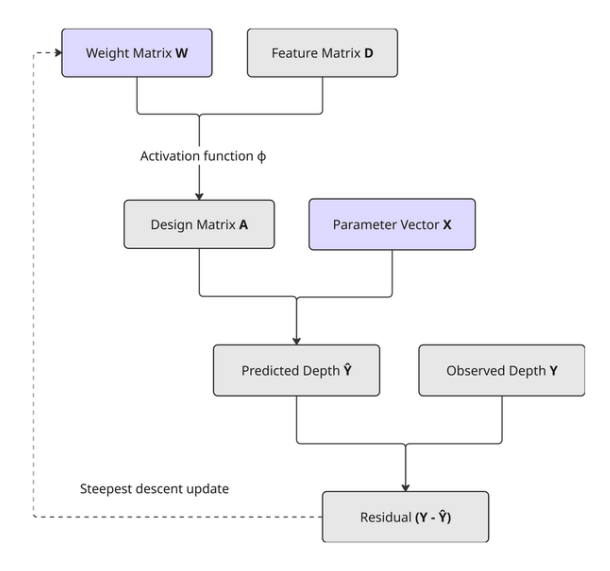


Figure 6. Schematic flowchart of the LSBDL model pipeline used for satellite-derived bathymetry.

In the implementation, the input vector consists of 12 Sentinel-2 spectral bands (B1–B12, excluding B10), with all band values normalized to the range [–1, 1]. Bathymetry output data, extracted from ICESat-2, is used to label the corresponding Sentinel-2 pixels, forming the training and validation datasets. An important step in data preparation involves outlier removal: after an initial model run, individual data points with residuals exceeding five meters were removed. These outliers predominantly occur around the outline of the island, likely due to inaccuracies in the Scene Classification Layer (SCL) of Sentinel-2, which may misclassify land pixels as water. Such misclassifications introduce bias into the training step, and thus were removed prior to further analysis.

The model architecture consists of a single hidden layer with n=50 neurons and a nonlinear 'sigmoid' activation function, followed by a linear output layer as described above. The dataset is randomly split, with 80% of the samples used for training and 20% for validation/testing to ensure robust spatial generalization. Training employs a learning rate of $\alpha=10^{-4}$, a softening parameter of s=0.5, and a momentum term of $\mu=0.9$ to iteratively update the weights W. A small regularization factor $\kappa=10^{-5}$ is used in the least-squares solution to stabilize the weight estimation X. This configuration, presented in Table 1, enables the LSBDL model to capture complex and nonlinear relationships in the data while preserving interpretability through explicit parameter-to-feature mapping. This offers a transparent and effective alternative to conventional "black-box" deep learning approaches for satellite-derived bathymetry.

A total of 42,823 data points were constructed by pairing 12-band Sentinel-2 imagery acquired on October 11, 2023, with

Par.	n	s	μ	α	κ	activation	Iter.
Val.	50	0.5	0.9	10^{-4}	10^{-5}	sigmoid	800

Table 1. Hyperparameter settings used for training the LSBDL model. Parameters include n: number of hidden layer neurons, s: softening parameter, μ : momentum parameter, α : learning rate, κ : regularization factor, activation function used, and number of training iterations.

co-located depth measurements derived from ICESat-2, resampled to a spatial resolution of 10 meters. These data were subsequently partitioned into training and validation subsets using an 80:20 split, resulting in 36,008 samples for training and 6,815 samples for validation.

Figure 7 presents the training and validation error curves over 800 iterations during the training of the LSBDL model. Both curves exhibit a steady decline in error and begin to level off around iteration 600, which indicates convergence. The small gap between the training and validation errors suggests that the model generalizes well to the validation data. Notably, there is no indication of significant overfitting or underfitting. As further indication, increasing / decreasing the number of hidden neurons to 100 / 25 did not result in a substantial improvement / deterioration in error, which suggests that the original model capacity was sufficient. A more detailed analysis of the model's performance will be provided in next section.

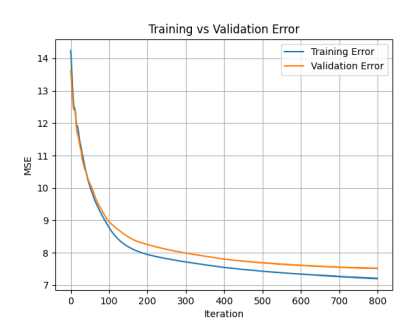


Figure 7. Training vs. validation error (measured in MSE) of the training process.

4. Results

The model outputs predicted depth values corresponding to the validation dataset. The performance metrics such as the coefficient of determination (\mathbb{R}^2) , root mean squared error (RMSE), and mean absolute error (MAE) were computed. In particular, the LSBDL model leverages the statistical foundations of least-squares theory to estimate the output covariance associated with the predicted depths. This output covariance serves as an uncertainty estimate, providing insight into the reliability of the model predictions.

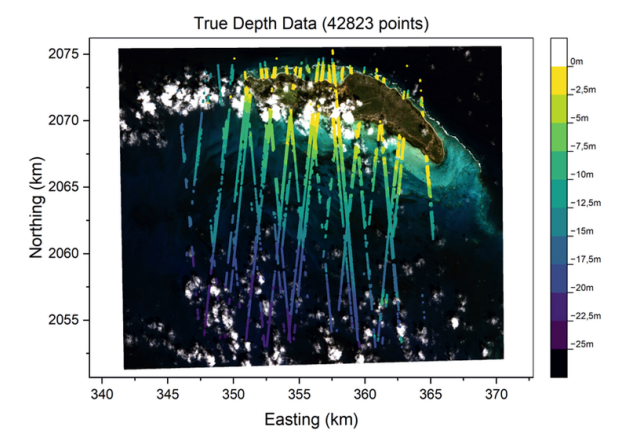
Table 2 presents the performance metrics of the LSBDL model. These results indicate that the model generalizes well to unseen data. Furthermore, the small difference between the MAE (2.28 m) and RMSE (2.74 m) suggests that the prediction errors are relatively consistent, with limited influence from extreme outliers. Overall, the model demonstrates robust and reliable predictive performance.

Figure 8 compares the true depth data for both the training and validation datasets, and the predicted depths for only the

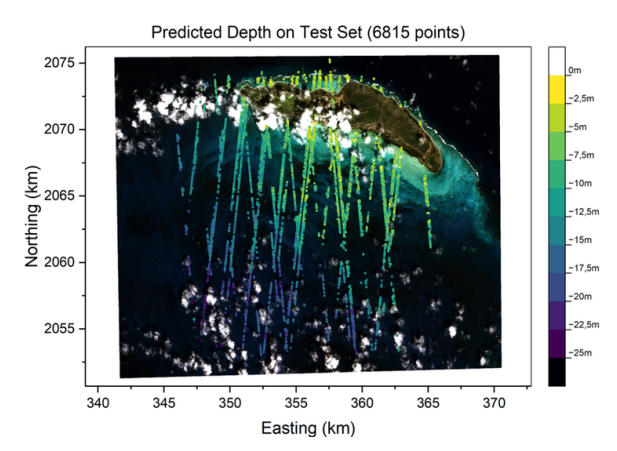
Met.	R^2	RMSE	MAE
Val.	0.75	2.74	2.28

Table 2. Performance metrics of the applied LSBDL model.

validation dataset. Overall, the depth values range from approximately 0 m to 25 m, with greater depths observed further from the island, which aligns well with expectations. However, a closer examination of the two depth maps reveals systematic discrepancies: in the shallow regions near the island, the predicted depths are generally overestimated, whereas in the deeper regions, particularly in the lower-left quadrant, the predicted depths tend to be underestimated compared to the true values.



(a) True depth data in study area, including both training and validation datasets. 42,823 data points in total

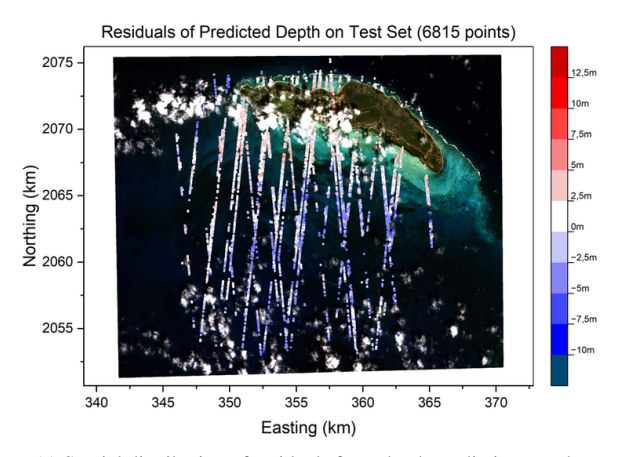


(b) Predicted depth on validation dataset. 6,815 data points in total.

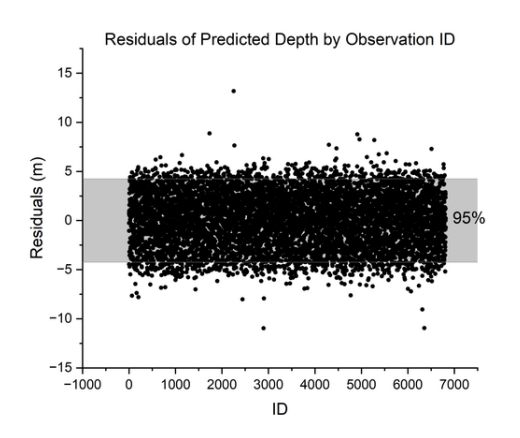
Figure 8. Comparison of true depths (a) and predicted depths on validation set (b).

To further elaborate on the previous statement, the prediction errors of the predicted depths (on validation data) are presented in Figure 9. As shown in Figure 9b, 95% of the residuals fall within approximately $\pm 4.7\,\mathrm{m}$, which indicates strong overall model performance and is smaller than the estimated 5.57 m standard deviation of the training data, suggesting that the model is making predictions with less variability than is inherent in the training dataset. However, the spatial distribution in Figure 9a reveals a clear pattern: overestimation (positive residuals) is concentrated in the shallow reef areas near the island, while underestimation (negative residuals) is more common in deeper offshore regions, particularly to the south and southwest.

Figure 10 illustrates the uncertainty of predicted depth using



(a) Spatial distribution of residuals from depth predictions on the validation dataset, overlaid on Sentinel-2 imagery acquired 11/10/2023.



(b) Residuals of depth predictions by observation ID on the validation dataset. The shaded gray area represents the interval within which 90% of the residuals fall, indicating the typical range of prediction errors.

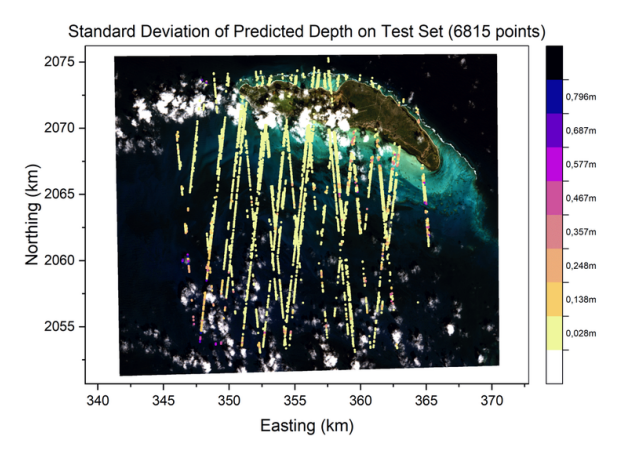
Figure 9. Residual analysis of depth predictions on the validation dataset.

the LSBDL model. This explains the standard deviation of the estimated depths, a well known metric to assess uncertainty in least squares solutions. The distribution across observation IDs (Figure 10b) reveals standard deviations ranging from 0 to 1. Given the amount of the available data, this suggests a high level of confidence in most model outputs with respect to random errors. The spatial distribution of prediction uncertainty (Figure 10a) highlights localized regions with higher uncertainties, particularly in the bottom-left and top-right parts of the study area. They may be attributed to factors such as lower data density, and hence limited training coverage in those regions, as well as potential effects like cloud occlusion.

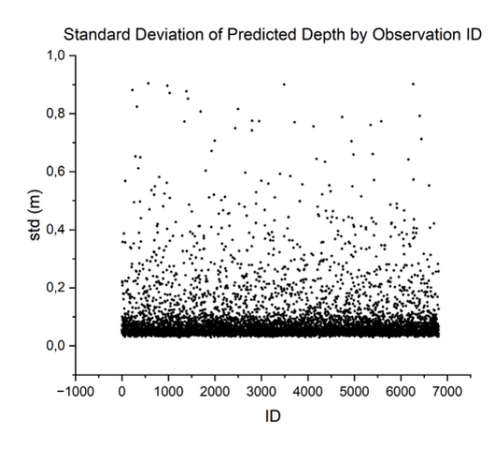
5. Discussion

The LSBDL model demonstrates strong performance for depths ranging from approximately 2–15 m, but its predictions become less reliable beyond 15 m, with increasing residual errors. This limitation is expected: at greater depths, the signal-to-noise ratio deteriorates due to light attenuation, a known constraint of passive SDB methods (Cesbron et al., 2021).

The residual error map (Figure 9a) reveals a systematic bias:



(a) Spatial distribution of standard deviation of depth predictions on the validation dataset, overlaid on Sentinel-2 imagery acquired on 11/10/2023



(b) Standard deviation of depth predictions by observation ID on the validation dataset.

Figure 10. Prediction standard deviation of depth estimates generated by the LSBDL model on the validation dataset.

the model tends to overestimate depth in shallow reef areas and underestimate it in deeper offshore regions. For example, a nearshore site exhibits larger residuals than a deeper offshore site, which suggests that factors beyond depth alone influence prediction accuracy. One possible explanation is that in shallow waters, darker benthic substrates—such as dense seagrass or coral shadows—reflect less light, making the water appear optically deeper (Casal et al., 2020; Towle, 2013). This can lead to depth overestimation in those areas. Addressing such effects will require further investigation to enhance the model's generalization and reduce systematic error.

A comparison between Figure 10a and Figure 9a reveals that the standard deviation of the predicted depth closely aligns with the residual distribution. Regions with high residuals, particularly in the lower-right area, also exhibit high predicted standard deviation. This correspondence suggests that the model's self-estimated standard deviation is a meaningful indicator of prediction uncertainty and represents a key advantage of the LSBDL framework. However, since the estimated standard deviations are generally smaller than the prediction errors (residuals), this suggests the presence of unmodeled effects in the modeling. For example, it can indicate that depth is likely not the sole factor influencing variations in the spectral bands. Other parameters, such as water clarity or bottom type, may

also need to be considered to improve the model's performance.

Our results indicated that using ICESat-2 data as the reference for true depths is effective, which eliminates the need for insitu calibration and enabling a fully satellite-based workflow. Although ICESat-2 depth points are sparser than traditional surveys, they provide a reliable and globally accessible source of bathymetric information.

Despite these strengths, the approach has several limitations. Most notably, the final RMSE of 2.74 m may be insufficient for applications requiring high precision, such as safe navigation. Additionally, the method remains constrained in waters deeper than 15 m, a challenge common to most SDB techniques. Lastly, reliance on ICESat-2 data imposes coverage constraints—particularly for applications that require high temporal resolution—due to the limited spatial density of available ground tracks.

6. Conclusion and Outlook

6.1 Conclusion

This study demonstrated a novel integration of neural networks with least-squares estimation for SDB, using Sentinel-2 imagery and ICESat-2 LiDAR data over Anegada's south coast. We showed that the LSBDL model can produce bathymetric maps with accuracy and consistency similar to traditional methods, while also providing enhanced interpretability through builtin uncertainty estimates. Key contributions of this work include: (1) applying the LSBDL framework to SDB for the first time, showing that it can give reliable depth predictions without site-specific calibrations; (2) demonstrating the practical use of freely available ICESat-2 photon-counting data as reference depths to train an SDB model over a 900 km² area, validating a cost-effective approach for mapping shallow seas; and (3) highlighting how interpretability from the least-squares theory can be leveraged to analyze residuals and quantify prediction confidence across the mapped area. In general, these findings advance the state-of-the-art in SDB by providing a technique that is not only accurate but also transparent. The outcomes are especially significant for data-sparse regions: coastal managers and scientists can now produce depth estimates with known confidence levels using only global satellite data, which is a substantial step forward in making coastal mapping more accessible and reliable.

6.2 Outlook

Building on this successful case study, there are several suggestions for future research to improve the applicability and robustness of the LSBDL approach for bathymetric mapping.

- 1. To improve the model's adaptation to turbid or optically complex waters, some additional inputs or modifications can be added to the LSBDL framework, for example, water quality indicators (turbidity estimates or colored dissolves organic matter indices) can be used as an additional input. Besides, physical-laws can be integrated into the model to account for light attenuation more explicitly.
- 2. Multisensor data or multi-image approaches can be explored to try extend the depth range the model is able to predict. For example, Sentinel-1 synthetic aperture radar (SAR) data can be utilized combined with wave-based depth inference.

3. Beyond this study area of Anegada, the LSBDL model can be tested in different water types, like tropical atolls or temperate estuaries, to validate its broad utility. New case studies can also reveal new challenges.

It is concluded that LSBDL has shown great promise for SDB, by combining the strengths of deep learning with the statistical rigor of least-squares. By addressing the limitations and pursuing the former-mentioned future directions, we may broaden the impact of LSBDL. We anticipate that this work has the potential to enhance coastal bathymetry mapping by improving confidence and scalability, thereby contributing to safer navigation, more effective coastal zone management, and a deeper scientific understanding of underwater environments.

References

Al Najar, M., Thoumyre, G., Bergsma, E. W., Almar, R., Benshila, R., Wilson, D. G., 2023. Satellite derived bathymetry using deep learning. *Machine Learning*, 112, 1107–1130.

Amiri-Simkooei, A., Tiberius, C., Lindenbergh, R., 2024. Deep learning in standard least-squares theory of linear models: Perspective, development and vision. *Engineering Applications of Artificial Intelligence*, 138, 109376.

Ashphaq, M., Srivastava, P. K., Mitra, D., 2021. Review of near-shore satellite derived bathymetry: Classification and account of five decades of coastal bathymetry research. *Journal of Ocean Engineering and Science*, 6(4), 340–359.

Bernardis, M., Nardini, R., Apicella, L., Demarte, M., Guideri, M., Federici, B., Quarati, A., De Martino, M., 2023. Use of ICEsat-2 and Sentinel-2 open data for the derivation of bathymetry in shallow waters: Case studies in Sardinia and in the Venice lagoon. *Remote Sensing*, 15(11), 2944.

Casal, G., Hedley, J. D., Monteys, X., Harris, P., Cahalane, C., McCarthy, T., 2020. Satellite-derived bathymetry in optically complex waters using a model inversion approach and Sentinel-2 data. *Estuarine, Coastal and Shelf Science*, 241, 106814.

Cesbron, G., Melet, A., Almar, R., Lifermann, A., Tullot, D., Crosnier, L., 2021. Pan-European Satellite-derived coastal bathymetry—review, user needs and future services. *Frontiers in Marine Science*, 8, 740830.

Eugenio, F., Marcello, J., Mederos-Barrera, A., Marqués, F., 2021. High-resolution satellite bathymetry mapping: Regression and machine learning-based approaches. *IEEE Transactions on Geoscience and Remote Sensing*, 60, 1–14.

European Space Agency, 2015. Sentinel-2 user handbook. https://sentinel.esa.int/documents/247904/685211/Sentinel-2_User_Handbook. Issue 1, Revision 2.

Kim, M., Danielson, J., Storlazzi, C., Park, S., 2024. Physics-based satellite-derived bathymetry (SDB) using Landsat OLI images. *Remote Sensing*, 16(5), 843.

Ma, Y., Xu, N., Liu, Z., Yang, B., Yang, F., Wang, X. H., Li, S., 2020. Satellite-derived bathymetry using the ICESat-2 lidar and Sentinel-2 imagery datasets. *Remote Sensing of Environment*, 250, 112047.

Najar, M. A., Benshila, R., Bennioui, Y. E., Thoumyre, G., Almar, R., Bergsma, E. W., Delvit, J.-M., Wilson, D. G., 2022. Coastal bathymetry estimation from Sentinel-2 satellite imagery: Comparing deep learning and physics-based approaches. *Remote Sensing*, 14(5), 1196.

Niroumand-Jadidi, M., Bovolo, F., Bruzzone, L., Gege, P., 2020. Physics-based bathymetry and water quality retrieval using planetscope imagery: Impacts of 2020 COVID-19 lockdown and 2019 extreme flood in the Venice Lagoon. *Remote Sensing*, 12(15), 2381.

Parrish, C. E., Magruder, L. A., Neuenschwander, A. L., Forfinski-Sarkozi, N., Alonzo, M., Jasinski, M., 2019. Validation of ICESat-2 ATLAS bathymetry and analysis of ATLAS's bathymetric mapping performance. *Remote Sensing*, 11(14), 1634.

Sutterley, T., 2023. YAPC: Yet another photon classifier. https://github.com/tsutterley/yapc. Accessed: 2025-05-19.

Towle, E. L., 2013. Island resources foundation. Technical report, Island Resources Foundation.

Xie, C., Chen, P., Zhang, S., Huang, H., 2024. Nearshore bathymetry from ICESat-2 LiDAR and Sentinel-2 imagery datasets using physics-informed CNN. *Remote Sensing*, 16(3), 511.